Polymer 50 (2009) 5987–5995

Contents lists available at ScienceDirect

Polymer

journal homepage: www.elsevier.com/locate/polymer

One pot synthesis of multiwalled carbon nanotubes reinforced polybenzimidazole hybrids: Preparation, characterization and properties

Huanzhen Shao, Zixing Shi*, Jianhua Fang, Jie Yin

School of Chemistry and Chemical Engineering, Shanghai Jiao Tong University, 800 Dongchuan Road, Shanghai 200240, People's Republic of China

ARTICLE INFO

Article history:
Received 17 July 2009
Received in revised form
25 September 2009
Accepted 19 October 2009
Available online 24 October 2009

Keywords:
Carbon nanotubes
One pot synthesis
Polybenzimidazole

ABSTRACT

Poly[2,2′-(p-oxydiphenylene)-5,5′-bibenzimidazole] (OPBI) nanocomposites containing 0.1–1 wt% multi wall carbon nanotubes (MWNTs) have been synthesized via "one pot synthesis" which combines the in situ modification of MWNTs and in situ polymerization of OPBI in one reaction pot, a technique that is particularly suitable for large scale production. Raman spectroscopy, NMR, XPS and XRD characterizations of OPBI grafted MWNTs (MWNT-g-OPBI), purified from the MWNT-g-OPBI/OPBI hybrid, reveal that the OPBI chains are successfully attached to the surface of MWNTs in the process of one pot synthesis method. Fracture morphology of the nanocomposites reveals very efficient distribution of the MWNTs within the OPBI matrix with good interfacial interaction. The mechanical properties (including tensile and yield strength, Young's modulus, etc.) are obviously increased even at 0.1 wt% MWNTs loading, and further improvement is observed at higher filler contents. The thermal stability and electrical conductivity are also improved with the incorporation of MWNTs.

1. Introduction

Carbon nanotubes (CNTs) (mainly single wall carbon nanotubes (SWNTs) and multi wall carbon nanotubes (MWNTs)) have attracted much attention in recent years because of their remarkable physical and chemical properties [1–4]. One of the most important potential applications is that it can be used as the ideal reinforcing agent for the high performance polymer based composites due to their tremendous mechanical strength, nanometer scale diameter and high aspect ratio [5–7]. However, the reinforcement is far away from that based on the theoretical calculation. Such behavior is due to the poor dispersion of CNTs in polymer matrix and the CNTs can only form aggregates in polymer matrix without exfoliation.

Thus, many efforts have been made to achieve homogeneous dispersion of CNTs in various matrix materials. Generally, there are two strategies (Scheme 1), one is non-covalent physical method aided by sonication or dispersants [8–17], and the other is the covalent attachment of chemical groups through reactions onto the π-conjugated skeleton of CNTs [18,19,25,26]. Solubilizing CNTs with suitable chemical groups attached to their surfaces can hinder close lateral contacts among the nanotubes, enable higher degrees of exfoliation, and allow isotropically reinforced nanocomposites to be prepared [20]. In this regard, the chemical modification of CNTs is more viable. Generally, the common approach for covalent modification of CNTs is that carboxylic acid groups are firstly introduced onto the surface of CNTs via strong acids (nitric acid) oxidation and then these acid groups are converted into other functional group by several complex reaction steps if needed. Although such conventional methods make great contribution to the improvement in the CNTs dispersion efficiency, they usually require very harsh reaction condition and lead to impairing the intrinsic morphology and properties of CNTs. Thus, developing an efficient as well as facile chemical modification method is desirable for preparing the carbon nanotube reinforced composites with high performance.

Tan research group [21–24] has proposed an efficient method for the modification of carbon nanotubes based on the Friedel–Crafts (F–C) reaction using polyphosphoric acid (PPA)/P_2O_5 as solvents. Such method has several advantages over the traditional modification method. The reaction medium (PPA) is a mild acid for effective purification and modification of CNTs with little structure destruction. The high viscosity of PPA can facilitate the good dispersion of CNTs with the minimum degree of aggregation. Such F–C acylation for CNTs functionalization and in situ polymerization using PPA as solvents can be combined together to produce the CNTs reinforced polymer hybrid just in one reaction pot. By this one reaction pot fashion, the modification of carbon nanotube and in situ polymerization can be designed to occur simultaneously or in continuous steps just in one reaction bottle without interruption for the purification of functional CNTs.

* Corresponding author. Tel.: +86 21 54743268; fax: +86 21 54747445.
E-mail address: zxshi@sjtu.edu.cn (Z. Shi).

0032-3861/$ – see front matter © 2009 Elsevier Ltd. All rights reserved.
doi:10.1016/j.polymer.2009.10.044

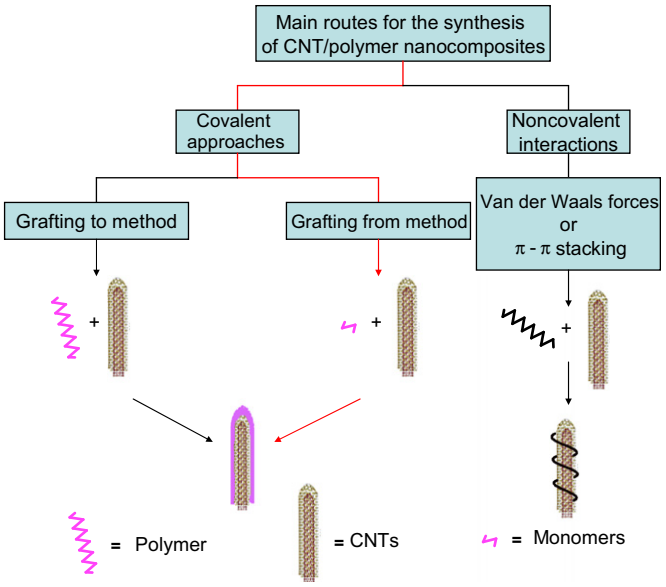

Scheme 1. Main routes for the synthesis of the CNTs/polymer nanocomposites. (Procedure of the red line is involved in the paper).

Here we report a novel "grafting from" approach [27] based on the in situ functionalization and dispersion of MWNTs in the PBI matrix in one reaction pot (one pot synthesis) (Scheme 2). Polybenzimidazole (PBI) is a kind of aromatic heterocyclic polymers containing benzimidazole units. Due to its high thermal and chemical stability properties, it is often used by fire departments and spaces agencies [28]. PBI has received much attention for its use as a high fuel cell membrane lately [29,30]. In order to improve the mechanical properties of PBI, several kinds of inorganic fillers, such as silica and montmorillonite, have been incorporated into the PBI matrix, but the reinforcement effect is not satisfactory [31]. Recently, our research group has successfully prepared the soluble PBI (OPBI) in methanesulfonic acid as solvents (the other kind of mild protonated acid) [32]. Good solubility of such polymer in high polar solvent makes it a potential candidate suitable for the preparation of MWNTs reinforced polymers in just one pot synthesis. In fact, it is found that the covalent linkage between MWNTs and polymer can be actually formed based on F–C reaction between MWNTs and carboxylic acid from the monomer in methanesulfonic acid as medium, which shows that the methanesulfonic acid is also good solvent for F–C reaction. As an extension of Tan's research work, we have designed "one pot synthesis" to prepare MWNT-g-OPBI/OPBI nanocomposites using methanesulfonic acid (instead of PPA) as solvent. This method excels in a relatively mild experimental condition, compared with previously strategies utilizing strong acids for the modification of the MWNTs, and shorter reaction time and relatively simple step, compared with Tan's method. Furthermore, such combination of the modification of MWNTs and in situ polymerization using methanesulfonic acid as medium, can be expected to provide the most effective reinforcement for PBI that could be applied to more severe conditions and new fields.

2. Experimental section

2.1. Materials

MWNTs (purity, >95%; length, ~10 μm; diameter, ~50 nm) were obtained from Chengdu Organic Chemistry Co., Ltd. 3,3′-Diaminobenzidine (DABz) was purchased from J&K Chemical in Shanghai and used without further purification. 4,4′-Dicarboxydiphenyl ether (DCDPE) was kindly supplied by Peakchem (Shanghai) and vacuum dried at 80 °C prior to use. Methanesulfonic acid (MSA), phosphorus pentoxide, dimethylsulfoxide (DMSO) were purchased from Sinopharm Chemical Reagent Co., Ltd (SCRC) and used as received.

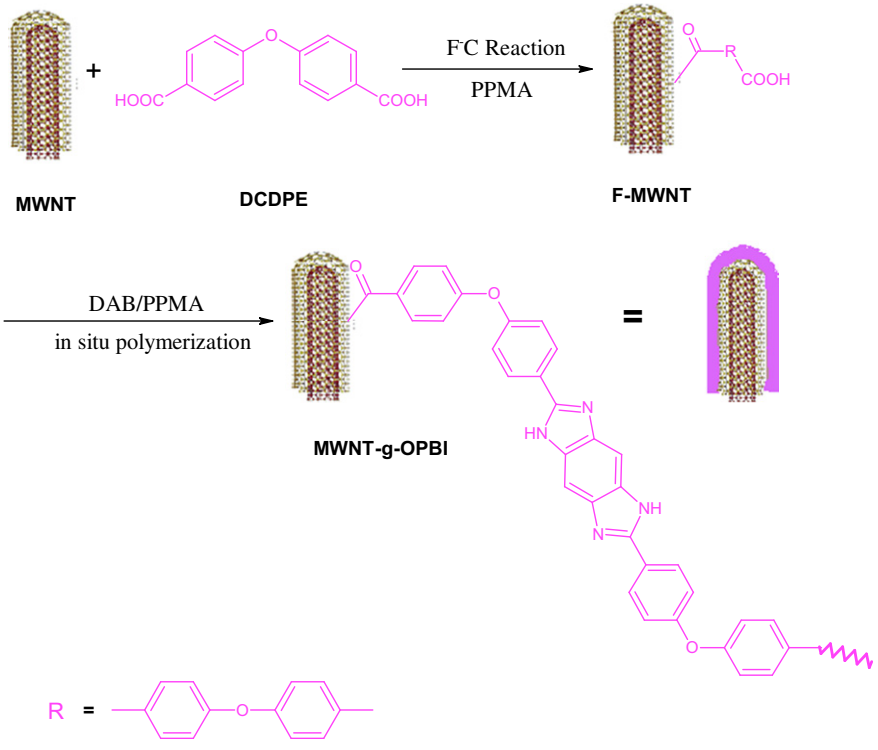

Scheme 2. Synthesis of the MWNT-g-OPBI/OPBI nanocomposite.

2.2. Measurements

^{1}H NMR spectra were recorded on a Varian Mercury Plus 400 MHz instrument. X-ray powder diffraction (XRD) spectra were acquired by D/max-2200/PC (Japan Rigaku Corporation) using Cu Kα radiation. Raman spectra were taken with Jobin Yvon Micro-Raman Spectroscopy (RamLab-010), equipped with a holographic grating of 1800 lines/mm and a He–Ne laser (632.8 nm) as excitation source. X-ray photoelectron (XPS) spectra were recorded on an ESCA LAB 250 spectrometer (VG Scientific) with an AlKα radiation (1486.6 eV). Thermogravimetric analysis (TGA) was performed in nitrogen with a Perkin–Elmer TGA 2050 instrument at a heating rate of 20 °C/min. For each measurement the sample cell was maintained at 100 °C for 30 min to evaporate the absorbed water in the sample before test. The cryo-fractured surface of composite, the morphology of functionalized MWNTs and MWNTs as received was obtained using FE-SEM (JSM-7401F, JEOL Ltd, Japan). FE-TEM images were obtained using JEOL2100F. Tensile measurements were performed with an Instron 4465 instrument in ambient atmosphere at a crosshead speed of 5 mm/min. Impedance analysis was recorded by using Autolab PGSTAT 302 electrochemical test system under frequency from 100 kHz to 10 Hz at room temperature using Alternating Current (AC).

2.3. Polymerization of MWNT-g-OPBI/OPBI nanocomposite

To a 100 ml dry three-neck flask, added as received MWNTs with different amounts (from 0.1 wt% to 1 wt%), DCDPE (5.0 mmol) and 45 g PPMA solution (phosphorus pentoxidel/methanesulfonic acid in a ratio of 1:10 by weight [33]). The reaction mixture was magnetically stirred under nitrogen flow in an ultrasonic bath for 1 h. It seemed MWNTs could disperse fairly well in PPMA. After the sonication, the mixture was kept at 100 °C for 4 h in an oil bath under stirring. Upon cooling to room temperature, DABz (5.0 mmol) was placed into the black solution, and the reaction mixture was heated to 140 °C for 40 min. Then it was slowly transferred to ice water with stirring. Whereafter, the silk like black product was soaked in 5% sodium bicarbonate solution under 60 °C for 36 h, then in deionized water for 3 h, and finally dried in vacuo at 120 °C.

For comparison, OPBI was prepared without adding MWNTs in the same procedure as above. The silk like product was brown and the yield was about 97% (2.28 g).

2.4. Preparation of MWNTs/OPBI nanocomposite

Just like the procedure for the synthesis of MWNT-g-OPBI/OPBI nanocomposite, MWNTs/OPBI nanocomposite was prepared as follows. To a 100 ml dry three-neck flask, added as received MWNTs with different amounts (0.1–1 wt%) and 45 g PPMA solution. The reaction mixture was magnetically stirred under nitrogen flow in an ultrasonic bath for 1 h. After the sonication, the mixture was kept at 100 °C for 4 h and then 140 °C for 40 min in an oil bath under stirring. Upon cooling to room temperature, 2.28 g OPBI was placed into the solution. After OPBI dissolved, the mixture was poured into water, soaked in 5% sodium bicarbonate solution under 60 °C for 36 h, then in deionized water for 3 h, and finally dried in vacuo at 120 °C.

2.5. Preparation of MWNT-g-OPBI

To make sure OPBI had already grafted from MWNTs, Soxhlet extraction was utilized to prepare MWNT-g-OPBI. MWNT-g-OPBI/OPBI nanocomposite was treated with DMSO in soxhlet extractor for 5 days to get rid of non-covalent OPBI. The resultant product was subsequently characterized by NMR, Raman spectroscopy, XRD, XPS, FE-SEM, FE-TEM and TGA.

2.6. Membrane formation

MWNT-g-OPBI/OPBI nanocomposites solution of 4–8 wt% in DMSO was sonicated for 15 min, and then cast onto glass plates and dried in an air oven at 80 °C for 5 h. The films were peeled off from glass plate and dried in vacuo at 120 °C for 10 h. The same procedure was applied to fabricate the MWNTs/OPBI membranes.

3. Results and discussion

3.1. Characterization of the functionalized MWNTs

FE-SEM was firstly applied to investigate the morphological structures of MWNTs and MWNT-g-OPBI obtained by refluxing with DMSO to remove the unattached OPBI prepared by one pot synthesis. Fig. 1 displays the FE-SEM images of MWNTs and MWNT-g-OPBI. For the raw MWNTs in Fig. 1(b), it was observed that the MWNTs surfaces were clean and the average diameter was in the range of 30–60 nm. In contrast, the surfaces of MWNT-g-OPBI were obviously coated with the polymer, as shown in Fig. 1(a), and the average diameter increased slightly, which was in the range of 40–80 nm.

TEM was also used to directly observe the OPBI layer wrapped around the MWNTs. Fig. 2 presents TEM images of MWNTs and MWNT-g-OPBI. As shown in Fig. 2(a), the convex surfaces of MWNTs seemed to be smooth with nothing adhering to them. In

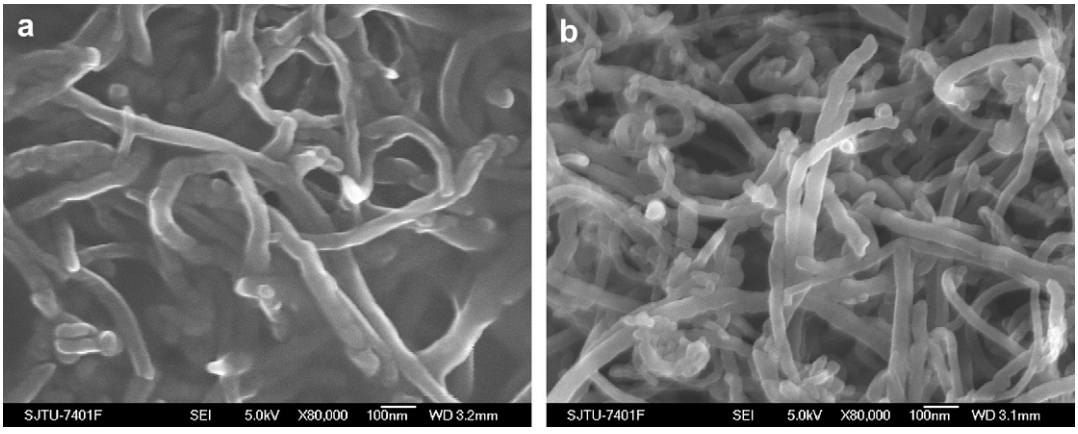

Fig. 1. SEM images: (a) MWNT-g-OPBI; (b) MWNTs

contrast, MWNT-g-OPBI had the core–shell structure (Fig. 2(b)). Fig. 2(c) and (d) show the further magnified TEM images of single MWNT and MWNT-g-OPBI. As can be seen in Fig. 2(c), the surface of the raw MWNT was smooth and its diameter was 40 nm. However, the surface of MWNT-g-OPBI was rough and fuzzy (Fig. 2(d)) owing to the outer wall of the MWNT coated with a polymer shell along the stretched direction of the tube and there is an obvious increase in the diameter as well and the polymer shell was not very even with a thickness from 3 to 10 nm.

Based on the analysis of combination of SEM and TEM images, it is found that the OPBI chains can be effectively attached to the surface of MWNTs by in situ compatibilization via F–C reaction from one pot synthesis.

The structure of MWNT-g-OPBI was also analyzed with NMR spectroscopy in detail. The ^{1}H NMR spectra of MWNT-g-OPBI and OPBI in deuterated DMSO are illustrated in Fig. 3. The resonance signals are mainly centered around 9–7 ppm, which are attributed to the benzene group, with a broad peak around 13 attributed to the proton of N–H from benzimidazole. There are six different kinds of aromatic protons, numbered from 1 to 6 in Fig. 3(a), centered at 7.31, 8.28, 7.66, 7.57, 7.83 and 13.01 ppm, respectively. Therefore, the peak assignment is just consistent with the chemical structures of OPBI polymer based on the NMR analysis. Compared of these spectra of pure OPBI and MWNT-g-OPBI, the following observations are obtained: (1) Spectra of MWNT-g-OPBI and OPBI show analogies of the corresponding signal patterns. (2) proton signals corresponding to the MWNT-g-OPBI are broader and lower intensities, as commonly observed in the NMR characterization of solubilized MWNTs [34]. Such comparison indicates that OPBI has been successfully grafted from MWNTs and MWNT-g-OPBI shows a good solubility in DMSO to form the homogeneous solutions, which is an important factor for successful NMR measurements.

Raman spectroscopy gives direct evidence for covalent sidewall functionalization in Fig. 4. Fig. 4(a) is the Raman spectra of as received MWNTs. The peak at 1327 cm^{-1} is called D band, which originates from the disordered graphite structure or sp^3-hybridized carbons of the nanotubes. While G band (1580 cm^{-1}) is attributed to a splitting of the E_{2g} stretching mode of graphite, which reflects the structural intensity of sp^2-hybridized carbon atoms [34]. In comparison, for MWNT-g-OPBI, the peaks at 1333 cm^{-1} and 1584 cm^{-1} are D band and G band, respectively. Obviously, both D band and G band show a spectral shift, which can be used to indicate sidewall or end-cap functionalization [35]. Meanwhile, G band is divided into two bands and the new band at a higher wavenumber (D') is also related to the extent of disorder in the nanotubes [36]. Furthermore, the relative intensity ratios of D to G

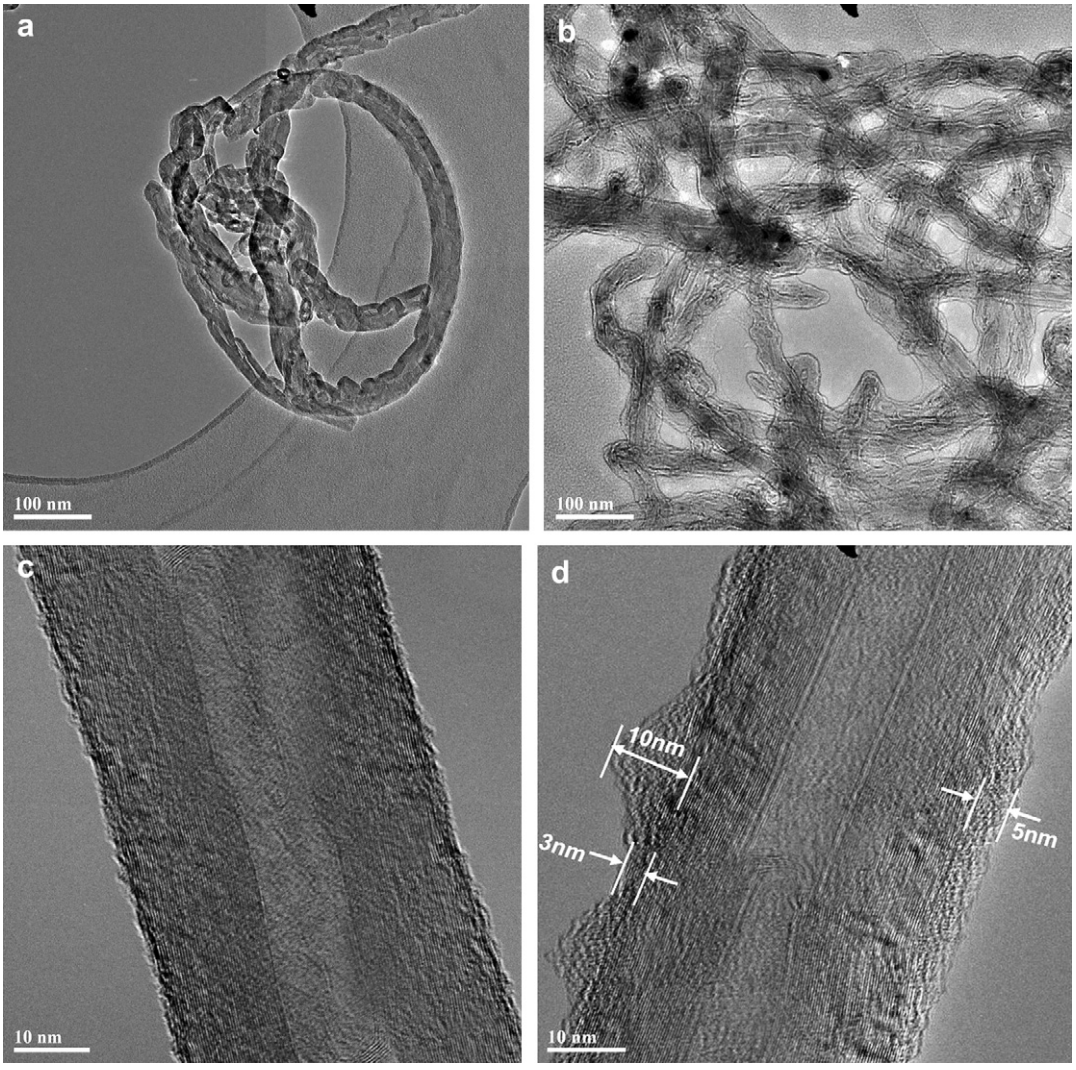

Fig. 2. TEM images: (a) MWNTs; (b) MWNT-g-OPBI. Scale bars are 100 nm. (c) MWNTs; (d) MWNT-g-OPBI. Scale bars are 10 nm.

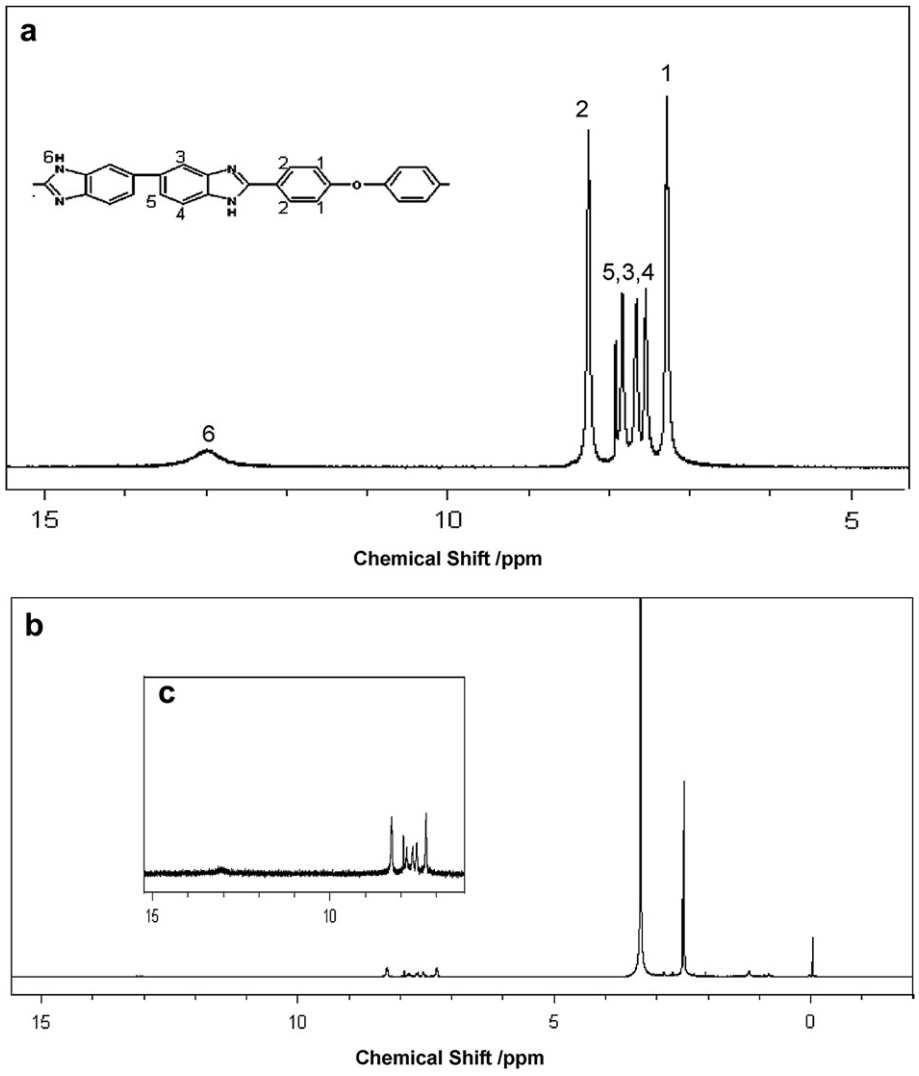

Fig. 3. ^{1}H NMR spectra of (a) OPBI, (b) MWNT-g-OPBI and (c) magnification of part of (b).

bands (I_D/I_G), utilized as an approach to monitoring the purity and functionalization of MWNTs, are 0.988 and 0.998 for MWNTs and MWNT-g-OPBI, individually. In conclusion, it is clear that OPBI has grafted from MWNTs.

To further confirm the successful grafting reaction, we also carried out powder X-ray diffraction (XRD) analysis. As shown in Fig. 5, the diffraction peaks at 26.5^0, 42.4^0 and 54.7^0 observed in the diffraction of MWNTs can be attributed to the hexagonal graphite

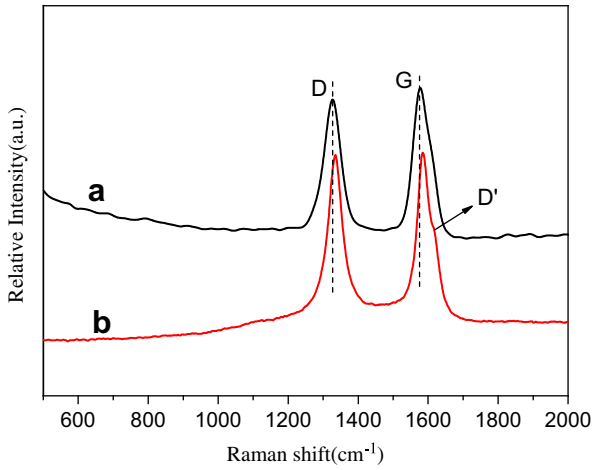

Fig. 4. Raman spectra of (a) MWNTs as received and (b) MWNT-g-OPBI.

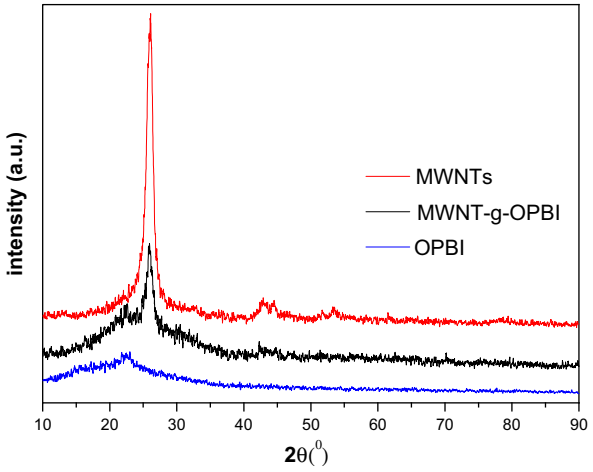

Fig. 5. XRD patterns of MWNT-g-OPBI, MWNTs and OPBI.

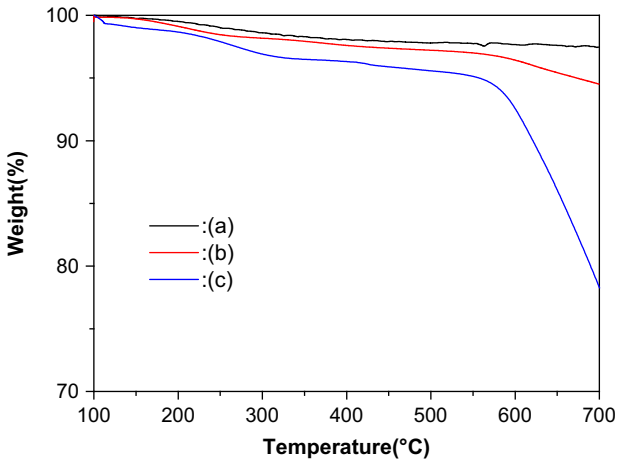

Fig. 6. TGA curves of (a) crude MWNTs; (b) MWNT-g-OPBI and (c) OPBI.

structures (002), (100) and (004) [37]. However, in addition to the nanotube reflection, MWNT-g-OPBI shows another weak peak at $2\theta = 22.5^{\circ}$, which is the reflection peak of the OPBI chains by comparison with the diffraction graph of the pure OPBI. The XRD data thus support that OPBI has been grafted from MWNTs.

TGA analysis was carried out to estimate the content of the OPBI chains grafted from the MWNTs surface. In order to eliminate the influence of water, all the samples were treated for 30 min under 100 °C before measuring. Fig. 6 shows the TGA curves of the MWNT, OPBI and MWNT-g-OPBI samples. It is clear that a small weight loss of 2.4% appear in Fig. 6(a), which is ascribed to the decomposition of deficient sites and carboxyl groups on the surface of the crude MWNTs. Compared with (a), because of the coating of OPBI chains, the functionalized MWNT displays obvious weight loss from 560 °C to 700 °C (about 6% at 700 °C). In addition, as shown in Fig. 6(b) and (c), the weight loss curves of the OPBI and MWNT-g-OPBI samples are much more alike. Therefore, we can derive that OPBI has successfully grafted from MWNTs. The polymer amounts grafted on MWNTs can be estimated about 27.3%.

XPS was utilized to individually elucidate the compositions of the MWNTs as received and MWNT-g-OPBI prepared from one pot synthesis. In each case, the gross elemental composition of the surface for the sample was established via an initial broad scan from 0 to 1350ev (Fig. 7(a) and (b). Both show a sharp carbon peak and a weak oxygen peak. However, compared with MWNTs (Fig. 7(a)), the oxygen peak of MWNT-g-OPBI becomes stronger. In the meantime, a new peak related to Nitrogen appears (Fig. 7(b)), revealing the successful graft of OPBI from MWNTs.

Furthermore, detailed analysis of the XPS spectra provides clear evidence that the grafting of OPBI from MWNTs has been achieved. As seen in Fig. 7, both (c) and (d) display peak intensity at 284.8 ev and 286.5 ev, which is originated from the sp^2 C═C, sp^3 C–C and C═O, C–O structures, respectively. However, (d) also includes a new peak, located at 286 ev, which was attributed to the C═N and C–N structures. This graph supplies evidence that OPBI has been successfully grafted from MWNTs.

3.2. Characterization of the nanocomposites

SEM was also applied to characterize the fracture surface of MWNTs reinforced polymer hybrids to evaluate the interfacial interaction between the MWNTs and polymer. Fig. 8(b), (d) and (f) show the fracture surface (broken under liquid nitrogen) of OPBI based hybrid containing different contents (0.1–1 wt%) of MWNTs prepared by one pot synthesis. For the MWNT-g-OPBI/OPBI nanocomposite with 0.1–0.5 wt% MWNTs, only few of broken MWNTs exist in the fracture surface and most of MWNTs

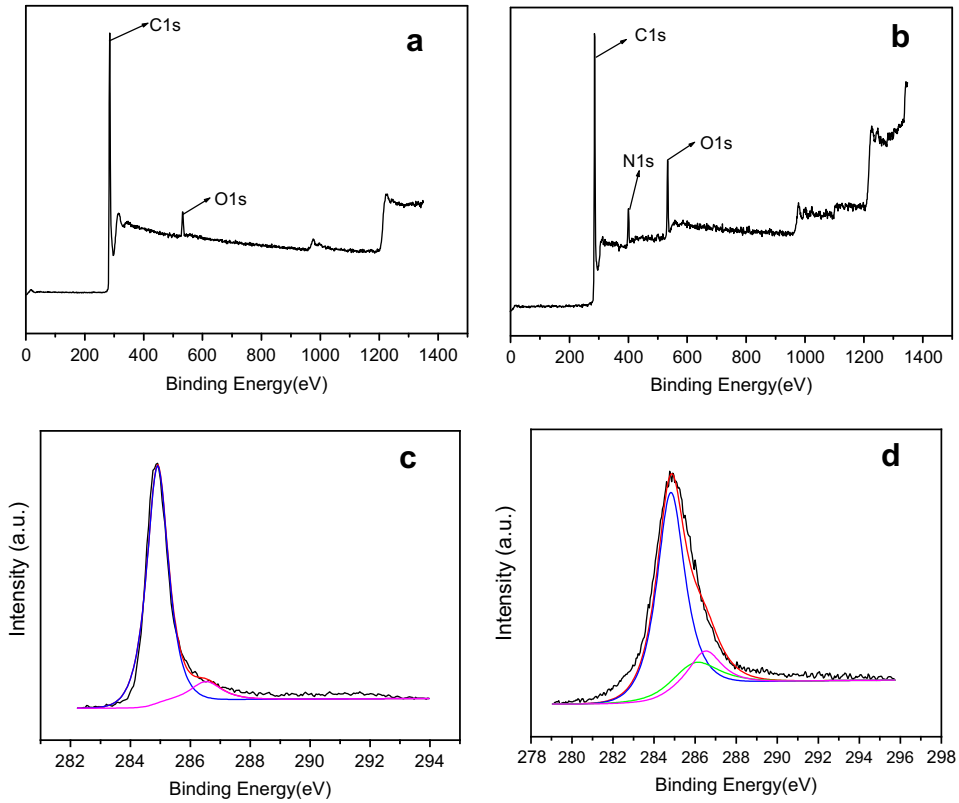

Fig. 7. XPS spectra: (a) wide scan spectrum and (c) C1s narrow scan spectrum of MWNTs as received; (b) wide scan spectrum and (d) C1s narrow scan spectrum of MWNT-g-OPBI.

are embedded within the OPBI matrix, indicating that the MWNTs show the homogeneous dispersion in OPBI matrix due to the formation of covalent bond between MWNTs and OPBI via in situ compatibilization in the process of one pot synthesis. As the MWNTs loading increases to 1 wt%, the number of ''broken'' MWNTs at the fracture interface increases and the surface of ''broken'' MWNTs is obviously coated with polymer layer. The exfoliation of MWNTs rather than aggregates is observed in the interface and most of them are in the ''broken mode'' instead of ''pull out mode''. Such observation suggests that even with relatively high MWNTs contents, the dispersion of MWNTs in OPBI matrix is still good and the aggregation of MWNTs is prevented by the repulsion force produced by the coated polymer on the surface of MWNTs.

The fracture interface for MWNTs/OPBI nanocomposites containing 0.1–1 wt% MWNTs produced by the physical blending is also illustrated for comparison in order to demonstrate the efficiency in the exfoliation of MWNTs in OPBI matrix. Fig. 8(a), (c) and (e) show the SEM images of the fracture interface for MWNTs/OPBI nanocomposites made by physical blends. It is found that most of the MWNTs are pulled out from the OPBI matrix due to the poor adhesion between MWNTs and polymer matrix. As the loading of MWNTs amounts to 1 wt%, it seems more MWNTs are retacked together as aggregates. Such observation indicates that physical blending method can not obtain the composites which have strong interface interaction between MWNTs and OPBI matrix and MWNTs are ready to aggregate. Therefore, MWNTs can be easily slipped from the OPBI matrix due to low interface interaction. In

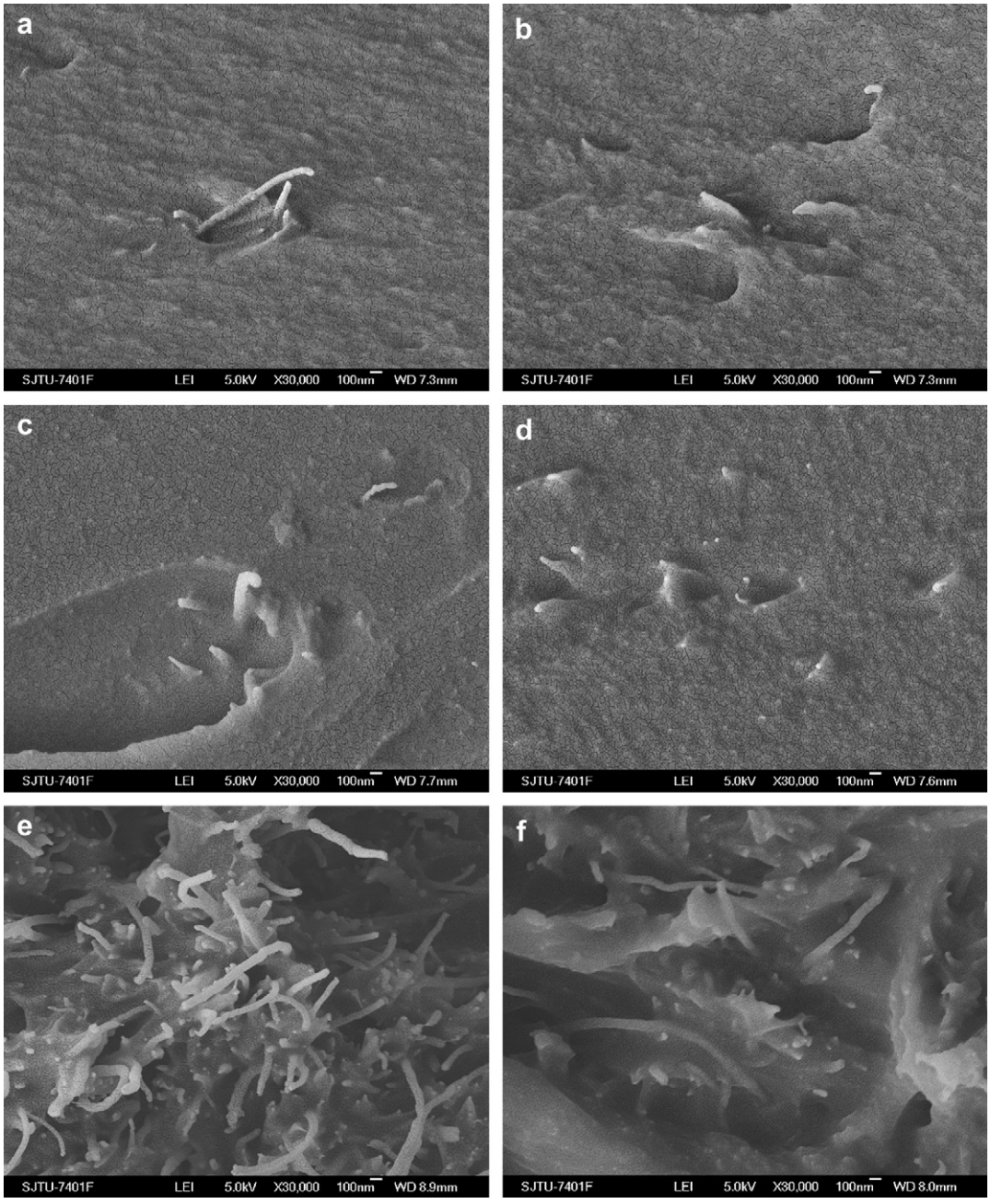

Fig. 8. SEM images of fractured surface: (a), (c), (e): 0.1%,0.5%,1% MWNTs/OPBI nanocomposites; (b), (d), (f): 0.1%,0.5%,1% MWNT-g-OPBI/OPBI nanocomposites.

contrast, as discussed above, there is strong interface interaction between the MWNTs and OPBI matrix in the MWNT-g-OPBI/OPBI nanocomposites. Well separated individual MWNTs prevails in the composites due to the repulsion force obtained by the attached polymer chains, so that, most of them are broken rather than pulled out from the interface. These micro-structural features of the composites have a strong connection with materials properties that will be discussed below.

MWNTs possess excellent mechanical properties such as high tensile strength and modulus. It is expected that incorporation of MWNTs at relatively low level loading can enhance mechanical properties for the polymer matrix significantly, if the problem of creating strong interfaces between MWNTs and polymer has been solved. Table 1 illustrates the results of the yield strength, tensile strength, young's modulus, and elongation-at-break for the two kinds of composites. For comparison, Fig. 9 illustrates their typical stress–strain curves for all the composites samples. It is found that MWNT-g-OPBI/OPBI hybrids prepared by one pot synthesis show obvious effective reinforcement for the OPBI matrix. The yield strength increases from 57 MPa for the pure OPBI to 70 MPa for the hybrids with 0.1 wt% loading of the MWNTs and its data progressively increases to 91 MPa as the content of the MWNTs increasing to 1%. The Young's modulus shows more than 40% improvement at just 1 wt% MWNTs content, compared with pristine OPBI. The tensile strength also increases simultaneously from 97 MPa to 138 MPa, as the MWNTs content rising from 0% to 1%. More attractively, the elongation-at-break is not compromised with the incorporation of MWNTs, which indicates that the ductility of film is retained with the incorporation of MWNTs. The result seems to be in conflict with the earlier report [38], in which the introduction of the short fibers into polymer matrix could reduce the ductility and toughness substantially. However, MWNTs present a special form of reinforcing fiber with high aspect ratio and greatly flexible elastic behavior. Additionally, retention or even improvement toughness can be achieved if the polymer chain is grafted to the surface of MWNTs resulting in the excellent dispersion of the MWNTs in the matrix.

For comparison, composites containing 0.1–1 wt% as received MWNTs prepared by physical blending are also studied and its data are summarized in Table 1. The addition of as received MWNTs improves the Young's modulus and yield strength. However, the enhancement is not so good as that brought by MWNT-g-OPBI. Similar to most of the results reported previously [25,26], both of the tensile strength and elongation-at-break decline with the addition of as received MWNTs into OPBI matrix. Such reduction in the mechanical properties may be due to the weak interfacial adhesion between MWNTs and OPBI matrix, which is observed in the fracture surface characterized by SEM. Besides, as the loading of the MWNTs increases, fairly poor dispersion occurs. As a result, the efficiency in load transfer from OPBI to MWNTs becomes lower.

In conclusion, good dispersion and strong interfacial adhesion accounts for the excellent mechanical properties. More specifically, with the chemical modification, long chemical moieties containing part of OPBI are attached onto the outer or defect sites of the MWNTs. They contribute to the uniform dispersion and good compatibility of MWNTs in the OPBI matrix.

Table 1
Mechanical properties of the nanocomposites.

Samples	Young's modulus (MPa)	Tensile Strength (MPa)	Elongation-at-break (%)	Yield Strength (MPa)
OPBI	2122	99	80.1	57
0.1%MWNT-g-OPBI/OPBI	2312	137	88.6	70
0.5%MWNT-g-OPBI/OPBI	2440	118	79.5	72
1%MWNT-g-OPBI/OPBI	2903	138	64.8	91
0.1%MWNTs/OPBI blend	2300	91	63.5	64
0.5%MWNTs/OPBI blend	2666	85	50.2	76
1%MWNTs/OPBI blend	2700	87	42.9	79

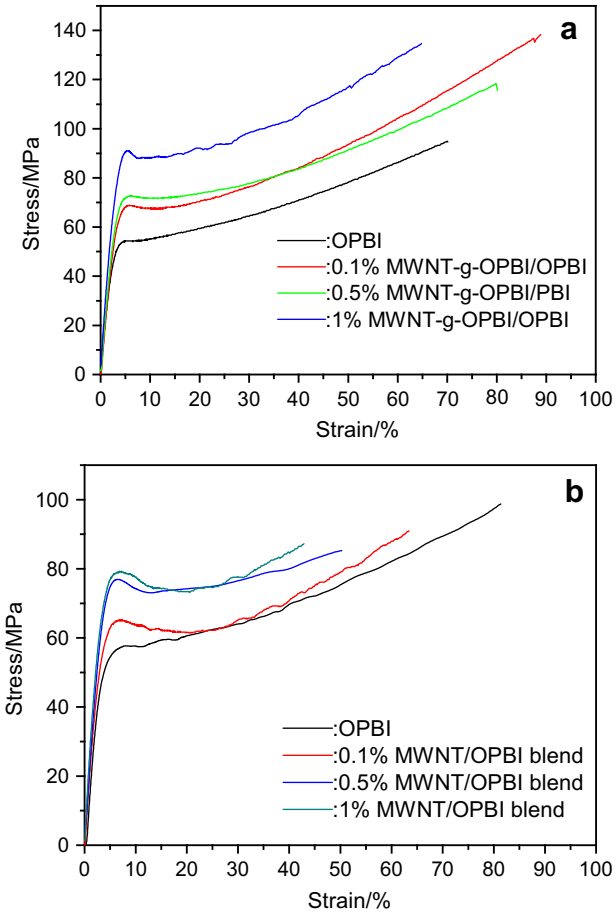

Fig. 9. Selected, representative stress–strain curves: (a) MWNT-g-OPBI/OPBI nanocomposites; (b) MWNTs/OPBI blend nanocomposites.

The hybrids with different content of MWNTs were subjected to thermogravimetric analysis (TGA) to determine their thermal stability in nitrogen. The results are depicted in Fig. 10. Overall,

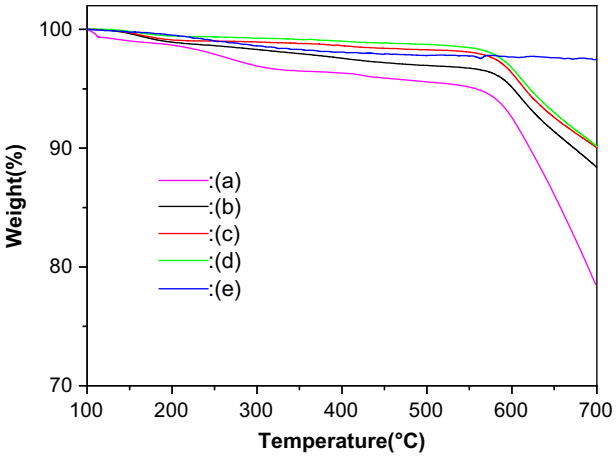

Fig. 10. TGA thermograms of nanocomposites in nitrogen with heating rate of 20 °C/min: (a) OPBI; (b) 0.1%MWNT-g-OPBI/OPBI; (c) 0.5%MWNT-g-OPBI/OPBI; (d) 1%MWNT-g-OPBI/OPBI; (e) MWNTs.

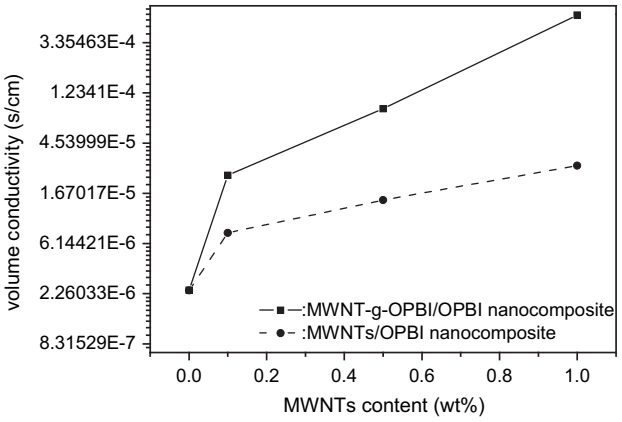

Fig. 11. AC conductivity plots of the MWNT-g-OPBI/OPBI nanocomposite (solid) and MWNTs/OPBI nanocomposite (dashed).

dynamic thermal stabilities of hybrids in nitrogen are much improved as indicated by the fact that the 5% weight loss temperatures ($T_{d5\%}$) for the hybrids containing 0.1%, 0.5%, 1 wt% MWNTs is 602, 615, and 622 °C, respectively, almost 50–70 °C increase as compared to 555 °C ($T_{d5\%}$) for the pure OPBI. Also, the char yields are also improved obviously for the sample with the incorporation of MWNTs. 0.1–1 wt% MWNTs addition can increase the char yields from 78% for the pure OPBI to about 88–90% for the hybrids, almost 10% increase in 700 °C.

MWNTs possess high aspect ratio and contain many π-bonds (C═C bond). The electrons will be transferred through the π-bonds (C═C bond) of MWNTs. Adding a small amount of MWNTs will improve the surface and volume conductivity significantly. Fig. 11 is the comparative plot of the AC conductivity of the MWNTs/OPBI nanocomposites as a function of the MWNTs content. It shows that the presence of MWNTs increases its conductivity for the samples prepared from one pot synthesis and physical blending. For the sample prepared from one pot synthesis, the volume conductivity is ascended to 2.39×10^{-5} s/cm by the incorporation of 0.1 wt% MWNTs. The volume conductivity was on the rise with increasing MWNTs contents. However, for sample fabricated via physical blending, the volume conductivity only increased to 7.59×10^{-6} s/cm by with the addition of 0.1 wt% MWNTs. Further accretion in MWNTs loading only resulted in slight increase in the volume conductivity. For example, the conductivity for sample containing 1 wt% MWNTs prepared by one pot synthesis increased to 5.8×10^{-4} s/cm, almost 20 times higher than that of the composite with the same content of MWNTs fabricated by the physical blending. Such big difference may be explained as follows: For the sample prepared by one pot synthesis, the well dispersed MWNTs in OPBI matrix facilitate the formation of conductive network in the OPBI matrix [39]. However, the aggregated carbon nanotubes in the OPBI hinder the formation of conductive path..

4. Conclusion

A facile method to prepare the MWNTs reinforced OPBI hybrid is proposed by combining the functionalization of the MWNTs and in situ polymerization in one reaction bottle, which is called "one pot synthesis". Such method has the advantage of reducing the conventional complex fabrication procedures and is particularly suitable for the bulk production of advanced polymer nanocomposites. Raman spectroscopy, SEM, TEM, XPS and ^{1}H NMR measurements show that the covalent bonding between MWNTs and OPBI is formed, resulting in the good dispersion of MWNTs in OPBI matrix. The composites obtained by this method exhibit obvious reinforcing effect in mechanical properties, including higher yield strength, tensile strength and enhanced young's modulus, as well as an improvement in the thermal stability and electrical conductivity

Acknowledgements

The authors thank the National Nature Science Foundation of China (No:50973062) for the support. Additionally, the authors also acknowledge the staff of Instrumental Analysis Center of Shanghai Jiao Tong University for the measurements.

References

[1] Treacy MMJ, Ebbesen TW, Gibson JM. Nature 1996;381:678–80.
[2] Ebbesen TW, Ajayan PM. Nature 1992;358:220–3.
[3] Ruoff RS, Lorents DC. Carbon 1995;33:925–30.
[4] Baughman RH, Zakhidov AA, de Heer WA. Science 2002;297:787–92.
[5] O'Connel MJ. Carbon nanotubes properties and applications. Boca Raton, FL: CRC Press; 2006. pp. 214.
[6] Calvert P. Nature 1999;399:210.
[7] Thostenson ET, Ren ZF, Chou TW. Compos Sci Technol 2001;61:1899–912.
[8] Okamoto M, Fujigaya T, Nakashima N. Adv Funct Mater 2008;18:1776–82.
[9] Nakashima N, Fujigaya T. Chem Lett 2007;36:692–7.
[10] Nakashima N, Tomonari Y, Murakami H. Chem Lett 2002;31:638–9.
[11] Murakami H, Nomura T, Nakashima N. Chem Phys Lett 2003;378:481–5.
[12] Nakashima N, Okuzono S, Murakami H, Nakai T, Yoshikawa K. Chem Lett 2003;32:456–7.
[13] Nakashima N. Int J Nanosci 2005;4:119–37.
[14] Muratami H, Nakashima NJ. Nanosci Nanotechnol 2006;6:16–27.
[15] Tomonari Y, Murakami H, Nakashima N. Chem Eur J 2006;12:4027–34.
[16] Nakashima N, Tanaka Y, Tomonari Y, Murakami H, Kataura H, Sakaue T, et al. Phys Chem B 2005;109:13076–82.
[17] Li XL, Liu Y, Fu L, Cao LC, Wang Y. Adv Funct Mater 2006;16:2431–7.
[18] Baskaran D, Mays JW, Zhang XP, Bratcher MSJ. Am Chem Soc 2005;127:6916–7.
[19] Sadowska K, Roberts KP, Wiser R, Biernat JF, Jablonowska E, Bilewicz R. Carbon 2009;47:1501–10.
[20] Lee H-J, Oh S-J, Choi J-Y, Kim JW, Han JW, Tan L-S, et al. Chem Mater 2005;17:5057–64.
[21] Baek J-B, Tan L-S. Polymer 2003;44:4135–47.
[22] Baek J-B, Lyons CB, Tan L-S. J Mater Chem 2004;14:2052–6.
[23] Han S-W, Oh S-J, Tan L-S, Baek J-B. Carbon 2008;46:1841–9.
[24] Eo S-M, Oh S-J, Tan L-S, Baek J-B. Eur Polym J 2008;44:1603–12.
[25] Tseng CH, Wang CC, Chen CY. Chem Mater 2007;19:308–15.
[26] Yang BX, Pramoda KP, Xu GQ, Goh SH. Adv Funct Mater 2007;17:2062–9.
[27] Tasis D, Tagmatarchis N, Bianco A, Prato M. Chem Rev 2006;106:1105–36.
[28] Choe EW, Choe DD. Polymer materials encyclopedia. Boca Raton, FL: CRC Press; 1996. p. 5619.
[29] Li QF, He RH, Jensen JO, Bjerrum NJ. Chem Mater 2003;15:4896–915.
[30] Bae JM, Honma I, Murata M, Yamamoto T, Rikukawa M, Ogata N. Sol State Ioni 2002;147:189–94.
[31] Choi SH, Coronas J, Lai ZP, Yust D, Onorato F, Tsapatsis MJ. Membr Sci 2008;316:145–52.
[32] Xu HJ, Chen KC, Gao XX, Fang JH, Yin J. Polymer 2007;48:5556–64.
[33] Ueda M, Sato M, Mochizuki A. Macromolecules 1985;18:2723–6.
[34] Du FP, Wu KB, Yang YK, Liu L, Gan T, Xie XL. Nanotechnology 2008;19:085716.
[35] Lefrant S, Baibarac M, Baltog I, Buisson J P, Chauvet O. Mol Cryst Liq Cryst Sci Technol A: Mol Cryst Liq Cryst 2002;374:325–34.
[36] Jorio A, Pimenta MA, Souza Filho AG, Saito R, Dresselhaus G, Dresselhaus M. New J Phys 2003;5:1–7.
[37] Zhou O, Fleming RM, Murphy DW, Chen CH, Haddon RC, Ramirez AP, et al. Science 1994;263:1744–7.
[38] Agarwal BD, Broutman LJ. Analysis and performance of fiber composites. New York: John Wiley&Sons; 1990.
[39] Li J, Ma PC, Chow WS, To CK, Tang BZ, Kim J-K. Adv Funct Mater 2007;17:3207–15.